

Efficient Hybrid Amplitude-Phase Quantization for Multi-Antenna Relay System

Changdae Kim, *Student Member, IEEE*, and Xianglan Jin, *Member, IEEE*

Abstract—This letter explores relay quantization in multi-antenna quantize-forward (QF) relay systems. Existing methods, such as uniform phase quantization (U-PQ) and uniform amplitude-phase quantization (U-APQ), suffer from performance saturation and high memory demands. To overcome these limitations, we propose hybrid amplitude-phase quantization (H-APQ), which adaptively quantizes received signal amplitudes based on their relative magnitudes while applying uniform quantization to individual phases. H-APQ significantly reduces memory consumption at the relay while maintaining strong overall performance, offering an efficient solution for multiple-input multiple-output (MIMO) QF relay systems.

Index Terms—Amplitude, multiple-input multiple-output (MIMO), quantization, relay

I. INTRODUCTION

Relay-assisted cooperative communication enhances wireless system performance by introducing an intermediate relay between a transmitter (source) and a receiver (destination) in a point-to-point (P2P) communication link. Traditional relay strategies include amplify-forward (AF) [1] and decode-forward (DF) [1], [2]. However, these methods have inherent limitations: AF relaying requires substantial memory to store continuous received signals, while DF relaying imposes high computational complexity due to the need for decoding and re-encoding. Additionally, both approaches rely on accurate channel estimation, further increasing system overhead.

Quantize-forward (QF) relaying provides a practical alternative by applying quantization to the received signals, significantly reducing memory requirements [3], [4], [5], [6], [7], [8]. Unlike AF and DF, QF does not require channel state information (CSI), making it well-suited for real-world communication scenarios with limited feedback. Moreover, it effectively addresses the drawbacks of AF and DF by reducing memory usage and computational complexity.

The most widely used quantization scheme in QF relay systems is uniform phase quantization (U-PQ), which quantizes and forwards only the phase information of the received signals [3], [4]. However, in multiple-input multiple-output (MIMO) QF relay systems, the performance of U-PQ saturates beyond a certain number of quantization bits [9]. This occurs because U-PQ accounts only for phase relationships between antennas while disregarding amplitude variations. To overcome this limitation, the uniform amplitude-phase quantization (U-APQ) algorithm was introduced in autoencoder-based relay

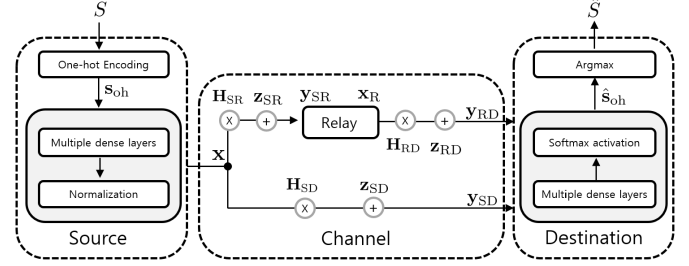


Fig. 1: An autoencoder-based QF relay system.

systems [9]. By incorporating both uniform phase quantization and uniform amplitude quantization, U-APQ outperforms U-PQ when using the same number of quantization bits. However, two key challenges remain: the amplitudes of the received signals are distributed over the range $(0, +\infty)$, requiring normalization prior to quantization. Additionally, because the normalized amplitudes are non-uniformly distributed within $(0, 1)$, with denser clustering in specific regions, they must be represented using a sufficiently large number of bits.

To address these issues, this letter proposes a novel hybrid amplitude-phase quantization (H-APQ) algorithm. While maintaining the same uniform phase quantization as U-APQ, H-APQ introduces a new amplitude quantization method, ordered amplitude quantization (O-AQ), which assigns quantization levels based on the relative magnitudes of received signal amplitudes. The proposed approach significantly reduces memory requirements while achieving comparable performance, making it an efficient solution for MIMO QF relay systems.

This letter is structured as follows. Section II describes the autoencoder-based QF relay system and reviews the existing U-PQ and U-APQ algorithms, followed by the introduction of the proposed H-APQ method. Section III presents numerical results demonstrating the effectiveness of H-APQ. Finally, Section IV concludes the letter.

II. AUTOENCODER-BASED QF RELAY SYSTEM

As illustrated in Fig. 1, we consider an autoencoder-based MIMO QF relay communication system¹. The autoencoder model comprises an encoder, a decoder, and a channel. In this

¹The proposed H-APQ can be applied to traditional communication systems that include channel encoding, modulation, demodulation, and decoding. However, we focus on an autoencoder-based relay system because the existing U-APQ method, to which H-APQ is compared, is designed specifically for autoencoder-based relay systems and cannot be applied in traditional communication frameworks.

relay cooperative communication system, the source functions as the encoder, while the destination serves as the decoder. The communication channel between the encoder and decoder includes the source-destination (SD) link, representing the direct path, and the source-relay-destination (SRD) link, which involves the relay.

In this section, we first describe the quantized relay channel, review existing quantization algorithms, and introduce a novel quantization algorithm. Finally, we provide a brief overview of the autoencoder-based relay system.

A. QF relay channel model

A relay cooperative communication system basically transmits a message from the source to the destination through the cooperation of the relay. The source, destination, and relay are equipped with N_S , N_D and N_R antennas, respectively.

In the first time slot, the source broadcasts symbols $\mathbf{x} = [x_1 \ x_2 \ \dots \ x_{N_S}]^T \in \mathbb{C}^{N_S}$ with $\|\mathbf{x}\|^2 = 1$ to the relay and destination. Then, the relay quantizes the received signals and stores the quantized information in memory.

In the second time slot where the source is in a waiting state, the relay generates new signals \mathbf{x}_R with $\|\mathbf{x}_R\|^2 = 1$ and transmits them to the destination after reloading the quantized information from the memory.

As a result, the received signals at the relay and destination for the first and the second time slots can be written

$$\mathbf{y}_{SR} = \mathbf{H}_{SR}\mathbf{x} + \mathbf{z}_{SR} \quad (1)$$

$$\mathbf{y}_{SD} = \mathbf{H}_{SD}\mathbf{x} + \mathbf{z}_{SD} \quad (2)$$

and

$$\mathbf{y}_{RD} = \mathbf{H}_{RD}\mathbf{x}_R + \mathbf{z}_{RD} \quad (3)$$

respectively, where $\mathbf{H}_{SR} \in \mathbb{C}^{N_R \times N_S}$, $\mathbf{H}_{SD} \in \mathbb{C}^{N_D \times N_S}$ and $\mathbf{H}_{RD} \in \mathbb{C}^{N_D \times N_R}$ represent the channel coefficient matrices for the source-relay (SR), SD, and relay-destination (RD) links, respectively. $\mathbf{z}_{kl} \sim \mathcal{CN}(0, \sigma^2 I_{N_l})$, $k \in \{S, R\}$, $l \in \{R, D\}$ are circularly symmetric complex Gaussian distributed noise vectors.

Then the transmission signal-to-noise ratio (SNR) for all links is $1/\sigma^2$.

B. Quantization algorithm at relay

1) *Uniform phase quantization (U-PQ) [3], [9]:* As shown in Fig. 2a, we perform q -bit U-PQ for each phase of the received signals at the relay in the first time slot. When the phase of the i th received signal satisfies $\frac{(2k-1)\pi}{2^q} < \angle[\mathbf{y}_{SR}]_i \leq \frac{(2k+1)\pi}{2^q}$, the quantized phase is obtained as

$$[\Theta_R]_i = \mathbf{Q}_q^{\text{U-PQ}}(\angle[\mathbf{y}_{SR}]_i) = \frac{2\pi k}{2^q} \quad (4)$$

where $k = 0, 1, \dots, 2^q - 1$ and $\mathbf{Q}_q^{\text{U-PQ}}(\cdot)$ is the element-wise U-PQ. At this point, the total number of required quantization bits is $N_b = qN_R$ to distinguish all the possible quantization levels.

As a result, we have

$$\mathbf{x}_R = \frac{1}{\sqrt{N_R}} e^{j\Theta_R} = \frac{1}{\sqrt{N_R}} e^{j\mathbf{Q}_q^{\text{U-PQ}}(\angle\mathbf{y}_{SR})} \quad (5)$$

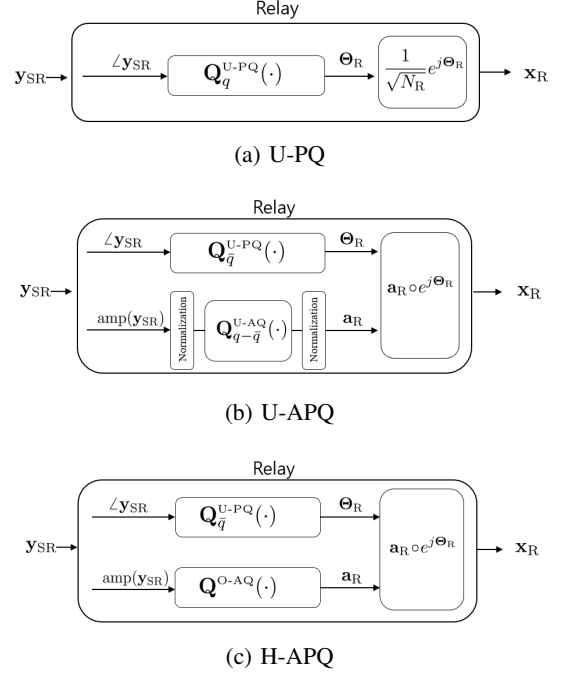


Fig. 2: Quantization algorithms at the relay.

where $e^{j\Theta_R} = [e^{j[\Theta_R]_1} \ \dots \ e^{j[\Theta_R]_{N_R}}]^T$ and each component is divided by $\sqrt{N_R}$ in order to satisfy the power constraint of $\|\mathbf{x}_R\|^2 = 1$.

In the MIMO QF relay system, performance improvement becomes limited when the number of quantization bits, q , exceeds a certain threshold [9]. This limitation stems from the difficulty in accurately forwarding the amplitude information of the received signals.

2) *Uniform amplitude-phase quantization (U-APQ) [9]:* As shown in Fig. 2b, the U-APQ algorithm quantizes both the amplitude and phase of the received signal at the relay with the same total number of bits as U-PQ. Among the q bits, \bar{q} bits are allocated to phase quantization denoted as $\mathbf{Q}_{\bar{q}}^{\text{U-PQ}}(\cdot)$, and $q - \bar{q}$ bits are allocated to amplitude quantization. Therefore, the total number of quantization bits is $N_b = qN_R$.

Since the amplitudes of the received signals are distributed over the range $(0, +\infty)$, the amplitudes of the N_R signals are first normalized. Then $q - \bar{q}$ bit uniform amplitude quantization (U-AQ), $\mathbf{Q}_{q-\bar{q}}^{\text{U-AQ}}(\cdot)$, is applied in the range of $(0, 1)$. After that, the normalization process is running again to satisfy the power constraint of $\|\mathbf{x}_R\|^2 = 1$. Finally, by combining the quantization information for the phases and amplitudes, the relay symbols vector \mathbf{x}_R is generated as

$$\mathbf{x}_R = \mathbf{a}_R \circ e^{j\Theta_R} \quad (6)$$

where \circ is an element-wise multiplication operation of vectors, $\Theta_R = \mathbf{Q}_{\bar{q}}^{\text{U-PQ}}(\angle\mathbf{y}_{SR})$ is the result of phase quantization. The vector \mathbf{a}_R is the final output of the amplitude component after normalizing the uniformly quantized amplitudes, $\mathbf{Q}_{q-\bar{q}}^{\text{U-AQ}}\left(\frac{\text{amp}(\mathbf{y}_{SR})}{\|\mathbf{y}_{SR}\|}\right)$. Here $\text{amp}(\mathbf{y}_{SR}) = [\alpha_1 \ \dots \ \alpha_{N_R}]^T$ is a vector containing the amplitudes of N_R received signals.

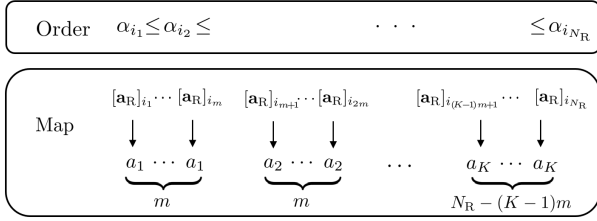


Fig. 3: Ordered amplitude quantization $\mathbf{Q}^{\text{O-AQ}}(\cdot)$.

Due to the non-uniform distribution of normalized amplitudes within $(0, 1)$, with higher density in certain regions, distinguishing amplitudes becomes challenging when fewer memory bits are used.

3) *Novel hybrid amplitude-phase quantization (H-APQ)*: To better distinguish amplitudes using fewer memory bits, we propose a H-APQ algorithm, which proceeds the same phase quantization $\mathbf{Q}_q^{\text{U-PQ}}(\cdot)$ as U-APQ, but introduces a novel amplitude quantization method called ordered amplitude quantization (O-AQ), as illustrated in Fig. 2c.

As depicted in Fig. 3, the O-AQ method first sorts the received signal amplitudes in ascending order, yielding the index sequence $\{i_1, i_2, \dots, i_{N_R}\}$ such that $\alpha_{i_1} \leq \alpha_{i_2} \leq \dots \leq \alpha_{i_{N_R}}$. Then, it assigns quantization levels from the ordered set $\mathcal{A} = \{a_1 < a_2 < \dots < a_K\}$, where each level is allocated to m amplitudes, ensuring a structured mapping of signal amplitudes to quantization levels. The number of quantization levels is determined as $K = \lceil N_R/m \rceil$. Larger amplitudes are assigned higher quantization levels, while smaller amplitudes receive lower ones. The detailed assignment process is as follows:

- The smallest m amplitudes, $\alpha_{i_1}, \dots, \alpha_{i_m}$, are assigned the smallest quantization level a_1 , i.e.,

$$[\mathbf{a}_R]_{i_1} = \dots = [\mathbf{a}_R]_{i_m} = a_1.$$

- The next m amplitudes $\alpha_{i_{m+1}}, \dots, \alpha_{i_{2m}}$ are quantized to a_2 , i.e.,

$$[\mathbf{a}_R]_{i_{m+1}} = \dots = [\mathbf{a}_R]_{i_{2m}} = a_2.$$

- This pattern continues for subsequent groups of m amplitudes.
- Finally, the remaining $N_R - (K-1)m$ largest amplitudes are assigned the highest quantization level a_K , i.e.,

$$[\mathbf{a}_R]_{i_{(K-1)m+1}} = \dots = [\mathbf{a}_R]_{i_{N_R}} = a_K.$$

This ensures a structured allocation of quantization levels based on the magnitudes of the received signal amplitudes.

Since the N_R signals transmitted after quantization must satisfy power constraint of $\|\mathbf{x}_R\|^2 = 1$, the components of $\mathcal{A} = \{a_1, a_2, \dots, a_K\}$ are subject to

$$\sum_{i=1}^{N_R} ([\mathbf{a}_R]_i)^2 = m \sum_{k=1}^{K-1} a_k^2 + (N_R - (K-1)m)a_K^2 = 1. \quad (7)$$

If the quantization levels are set as $a_k = k\Delta$ for $k = 1, \dots, K$, the power constraint in (7) determines Δ as

$$\Delta = \sqrt{\frac{1}{\frac{m(K-1)K(2K-1)}{6} + (N_R - (K-1)m)K^2}}. \quad (8)$$

This ensures that the quantization set $\mathcal{A} = \{\Delta, 2\Delta, \dots, K\Delta\}$ satisfies (7). While this case adopts $a_k = k\Delta$ as the quantization levels, other level selection strategies that meet the power constraint in (7) can also be applied in the O-AQ method. Thus, unlike U-APQ, the H-APQ method does not require two normalization steps in the amplitude quantization process.

As a result of H-APQ, \mathbf{x}_R can also be written as the form in (6), where $\Theta_R = \mathbf{Q}_q^{\text{U-PQ}}(\angle \mathbf{y}_{\text{SR}})$ is the same one in (6), and \mathbf{a}_R is the result of O-AQ.

In O-AQ, the number of possible quantized amplitude vectors, \mathbf{a}_R , is

$$\begin{aligned} & \binom{N_R}{m} \binom{N_R - m}{m} \dots \binom{N_R - (K-1)m}{N_R - (K-1)m} \\ &= \frac{N_R!}{(N_R - (K-1)m)!(m!)^{K-1}}. \end{aligned} \quad (9)$$

Consequently, the number of bits required to distinguish the quantized amplitude information is $\lceil \log_2 \left(\frac{N_R!}{(N_R - (K-1)m)!(m!)^{K-1}} \right) \rceil$, and this value decreases as m increases. As a result, the total number of quantization bits required for H-APQ is $N_b = \bar{q}N_R + \lceil \log_2 \left(\frac{N_R!}{(N_R - (K-1)m)!(m!)^{K-1}} \right) \rceil$.

Table I provides a summary of the number of quantization bits required for the three quantization methods at the relay.

TABLE I: Number of quantization bits.

	U-PQ	U-APQ	H-APQ
# of bits	qN_R	qN_R	$\bar{q}N_R + \lceil \log_2 \left(\frac{N_R!}{(N_R - (K-1)m)!(m!)^{K-1}} \right) \rceil$

C. Autoencoder-based communication system

We transmit a message $S \in \mathcal{M} = \{1, 2, \dots, M^{N_s}\}$ from the source to the destination, as shown in Fig. 1. To facilitate this, we employ an end-to-end autoencoder and a submessage one-hot encoding scheme [9]. First, the message S is transformed into a one-hot encoded vector \mathbf{s}_{oh} , which is then processed through multiple dense layers and normalized to produce the signal \mathbf{x} . The signal \mathbf{x} is transmitted to the QF relay channel using N_S antennas as described in Section II-A. At the destination, the received signals, \mathbf{y}_{SD} and \mathbf{y}_{RD} , are input into a decoder comprising multiple dense layers with softmax activation. The decoder outputs an estimate of the one-hot encoded vector, $\hat{\mathbf{s}}_{\text{oh}}$.

In this autoencoder model, the training process minimizes the categorical cross-entropy loss between the true one-hot encoded vector \mathbf{s}_{oh} and its estimation $\hat{\mathbf{s}}_{\text{oh}}$. During the test phase, the final estimated value \hat{S} is determined as the index of the component with the maximum probability in $\hat{\mathbf{s}}_{\text{oh}}$.

III. NUMERICAL RESULT

In Section II, we introduced the H-APQ algorithm as a memory-efficient quantization method for MIMO QF relay channels. This section compares its performance against existing quantization methods.

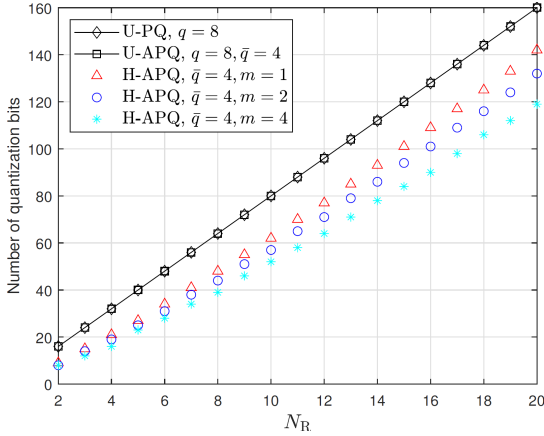


Fig. 4: Number of quantization bits for various quantization methods at the relay.

A. Memory requirement at relay

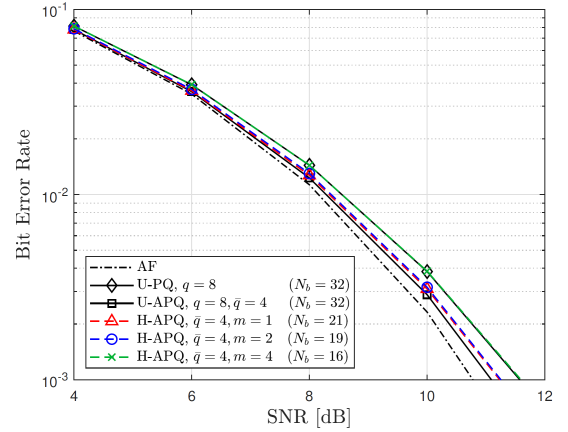
Since the comparison of required quantization bits in Table I may not be sufficiently intuitive, we provide an illustration for better visualization. Figure 4 illustrates that U-PQ with $q = 8$ and U-APQ with $q = 8, \bar{q} = 4$ require the highest memory usage. In contrast, H-APQ significantly reduces memory consumption, particularly for larger values of m . Even when $m = 1$ (denoted by \triangle markers), H-APQ remains more memory-efficient than other methods for $N_R \leq 20$. This highlights how H-APQ effectively saves memory usage by adjusting the parameter m unlike conventional quantization methods.

B. System performance

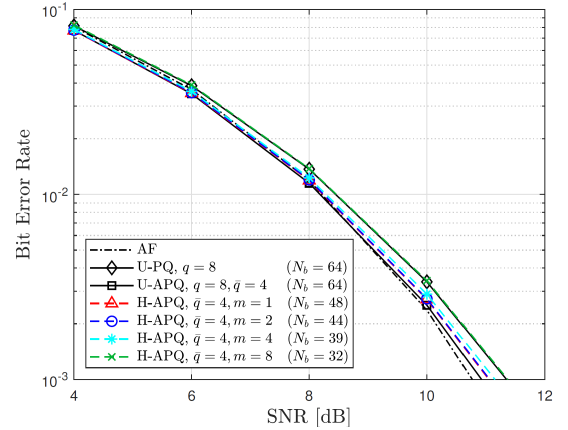
The deep learning models are trained using the Adam optimizer [10] within the TensorFlow framework [11]. To evaluate the bit error rate (BER), we assume Rayleigh fading channels, i.e., $\mathbf{H}_{kl} \sim \mathcal{CN}(0, I_{N_l})$, $k \in \{S, R\}$, $l \in \{R, D\}$, for both training and test. For $N_S = 4$, we use a training dataset of $N_{\text{train}} = 10^5$. As the model size increases, the dataset is expanded to $N_{\text{train}} = 2 \times 10^5$ for $N_S = 8$ and $N_{\text{train}} = 3 \times 10^5$ for $N_S = 16$ to accommodate the larger model.

1) *H-APQ with $a_k = k\Delta$* : Figure 5 illustrates the BER performance of autoencoder-based MIMO QF relay systems with $M = 4$ for different quantization methods where H-APQ employs $a_k = k\Delta$. The ‘‘AF’’ curve represents the autoencoder-based MIMO AF relay system, serving as the performance benchmark. The key observations are as follows:

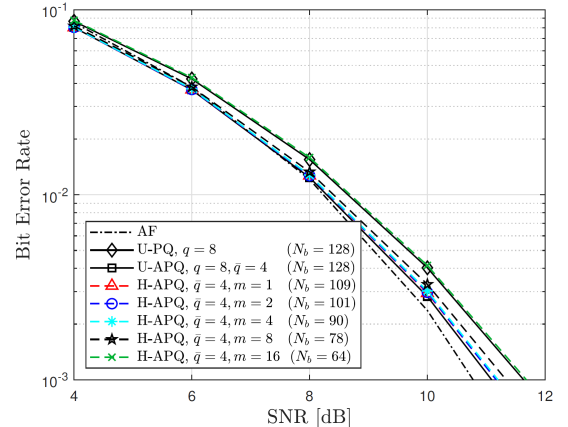
- U-APQ with $q = 8, \bar{q} = 4$ achieves the best performance, closely approaching AF. However, this comes at the cost of high memory usage ($N_b = 32$ for $N_R = 4$, $N_b = 64$ for $N_R = 8$, and $N_b = 128$ for $N_R = 16$).
- U-PQ with $q = 8$, despite using the same number of quantization bits as U-APQ, performs the worst.
- H-APQ with $m = N_R$, equivalent to U-PQ with $q = 4$, performs similarly to U-PQ with $q = 8$, highlighting the performance saturation of U-PQ as the number of quantization bits increases.



(a) $N_S = N_R = N_D = 4$



(b) $N_S = N_R = N_D = 8$



(c) $N_S = N_R = N_D = 16$

Fig. 5: BER comparison for various quantization algorithms in the autoencoder-based MIMO QF relay systems with $M = 4$, where H-APQ applies $a_k = k\Delta$.

- H-APQ with $m < N_R$ achieves intermediate performance. Notably, H-APQ with $m = 2$ offers near-optimal performance close to U-APQ while significantly reducing memory usage, by up to 13 bits for $N_R = 4$, 20 bits for $N_R = 8$, and 27 bits for $N_R = 16$. Moreover, as N_R increases, the performance of H-APQ with $m = 2$

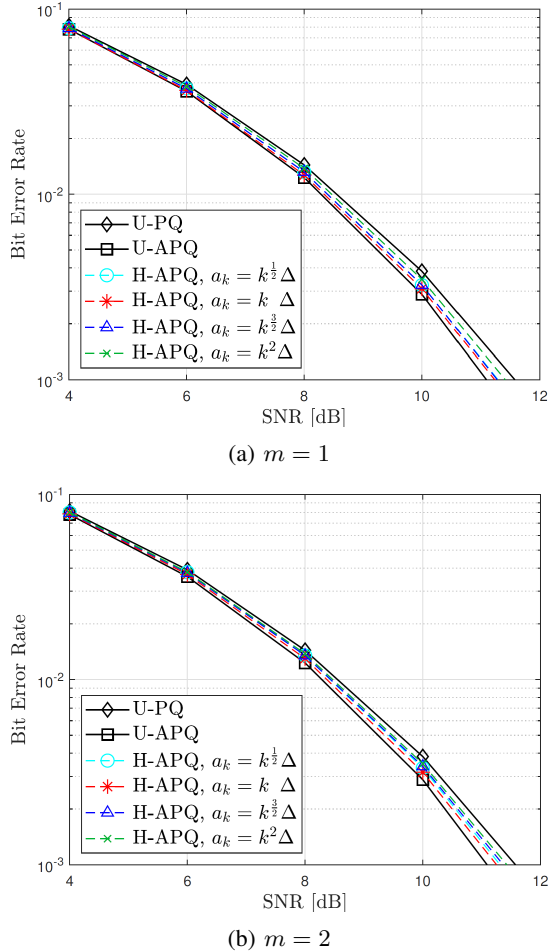


Fig. 6: BER comparison for H-APQ with various kinds of quantization levels, a_k , when $N_S = N_R = N_D = 4$ and $M = 4$.

progressively converges to that of U-APQ.

These findings demonstrate that H-APQ effectively balances performance and memory constraints. Furthermore, by appropriately selecting m , the method can optimize performance while accommodating the relay's memory constraints.

2) *H-APQ with different a_k configurations*: As discussed in Section II-B3, various quantization levels can be applied in the O-AQ method. Figure 6 compares BER performance for $N_S = N_R = N_D = 4$ and $M = 4$ when different quantization levels are used: $a_k = k^{\frac{n}{2}} \Delta$ with $n = 1, 2, 3, 4$. The “U-PQ” and “U-APQ” curves, corresponding to the cases $q = 8$ and $q = 8, \bar{q} = 4$, respectively, serve as reference points for performance evaluation. One can observe that:

- The BER curves for all cases fall between U-PQ ($q = 8$) and U-APQ ($q = 8, \bar{q} = 4$).
- $a_k = k \Delta$ achieves the best performance, while $a_k = k^2 \Delta$ performs the worst.
- $a_k = k^{\frac{1}{2}} \Delta$ and $a_k = k^{\frac{3}{2}} \Delta$ exhibit similar intermediate performance.

These results indicate that evenly spaced quantization levels, i.e., $a_k = k \Delta$, yield excellent performance, although they may not always be optimal. Conversely, if spacing between quantization levels either decreases or increases with k , distin-

guishing amplitude levels becomes more challenging, leading to degraded performance.

Finally, modifying the quantization levels for O-AQ does not alter the number of required quantization bits. Thus, H-APQ with alternative quantization levels still offers significant memory savings over U-PQ and U-APQ, allowing for adaptive application based on system characteristics.

IV. CONCLUSION

This letter introduced the H-APQ algorithm, which integrates the O-AQ method for amplitude quantization, adaptively quantizing received relay signal amplitudes based on their relative magnitudes. While U-PQ experiences performance saturation even with increased quantization bits and U-APQ improves performance at the cost of high memory usage, H-APQ effectively balances these trade-offs. Additionally, we examined various quantization-level strategies for O-AQ and demonstrated that evenly spaced quantization levels can achieve strong performance. By significantly reducing memory requirements at the relay while maintaining competitive overall performance, H-APQ offers a practical and efficient solution for MIMO QF relay systems.

REFERENCES

- [1] J. N. Laneman, D. N. C. Tse and G. W. Wornell, “Cooperative diversity in wireless networks: Efficient protocols and outage behavior,” *IEEE Trans. Inf. Theory*, vol. 50, no. 12, pp. 3062–3080, Dec. 2004.
- [2] X. Jin, J.-S. No, and D.-J. Shin, “Relay selection for decode-and-forward cooperative network with multiple antennas,” *IEEE Trans. Wireless Commun.*, vol. 10, no. 12, pp. 4068–4079, Dec. 2011.
- [3] M. Souryal and H. You, “Quantize-and-forward relaying with M-ary phase shift keying,” *2008 IEEE Wireless Commun. and Netw. Conference, Las Vegas, NV*, pp. 42–47, Apr. 2008.
- [4] X. Jin, “Cooperative linear combining on quantize-forward relay channel with M-ary phase shift keying,” *IEEE Trans. Veh. Technol.*, vol. 71 no. 5, pp. 5645–5650, May 2022.
- [5] J. Park and X. Jin, “Low-complexity linear signal detection on two-way quantize-forward relay channel,” *IEEE Wireless Commun. Letters*, vol. 12, no. 12, pp. 2208–2212, Dec. 2023.
- [6] A. Steiner and S. S. Shamai, “Single-user broadcasting protocols over a two-hop relay fading channel,” *IEEE Trans. Inf. Theory*, vol. 52, no. 11, pp. 4821–4838, Nov. 2006.
- [7] X. Jin, “Amplify-quantize-forward relay channel with quadrature amplitude modulation,” *IEEE Access*, vol. 10, pp. 89445–89457, 2022.
- [8] X. Jin, “MIMO detection on amplify-quantize-forward relay channel,” *IEEE Trans. Veh. Technol.*, vol. 73, no. 6, pp. 8473–8486, Jun. 2024.
- [9] J. Shin and X. Jin, “Autoencoder-based MIMO cooperative communications with quantize-forward relaying,” *IEEE Trans. Vehicular Technology*, vol. 73, no. 12, pp. 19229–19239, Dec. 2024.
- [10] D. Kingma and J. Ba, “Adam: A method for stochastic optimization,” *arXiv preprint arXiv:1412.6980*, 2014.
- [11] M. Abadi, A. Agarwal, P. Barham, E. Brevdo, Z. Chen, C. Citro, G. S. Corrado, A. Davis, J. Dean, M. Devin, et al., “Tensorflow: Large-scale machine learning on heterogeneous distributed systems,” *arXiv preprint*, 2016. url = <http://arxiv.org/abs/1603.04467>